E-ISSN: 3107-5843
International Journal of Advanced Engineering and Management System
Volume 01, Issue 01, April-June 2025, pp. 74 - 83

A MULTI PORT DC TO DC CONVERTER FOR PV/BATTERY/DC GRID ENERGY SYSTEM

Preethi Balachander[1], Department of Artificial Intelligence and Data Science, SRM College Of Engineering Technology, Chennai, India (e-mail: preethithara12@gmail.com)

Bakkialakshmi V S[2], Department of Computing Technologies, Faculty of Engineering Technology, SRM College Of Engineering Technology, Chennai, India (e-mail: bakkyam30@gmail.com)

Abstract:

In accordance with the growing need for power conversion systems that are efficient and multifunctional, this project introduces a multi-port DC-DC converter that integrates photovoltaic (PV) panels, batteries, and DC grids. The system designed in this approach includes a Single-Ended Primary Inductor Converter (SEPIC), a bi-directional converter, and an inverter circuit, providing continuous energy management. The SEPIC converter steps up or steps down the input voltage efficiently to ensure a stable power supply. The bi-directional converter allows for power exchange between the battery and the grid to support controlled discharging and charging operations. The inverter module also converts DC power to AC, which makes the system applicable to traditional AC loads. The multi-port architecture increases the flexibility of the system, allowing optimal power distribution between multiple energy sources and enhancing the overall efficiency and reliability. This is the best solution for renewable energy use, smart grid, and hybrid energy storage devices, leading to sustainable and resilient power management.

Keywords: Multi-Port Converter, SEPIC Converter, Bi-Directional Converter, DC-AC Inverter, Renewable Energy Integration, Battery Energy Management.

1. Introduction

The industrial process extension has become extremely complex in the current trending electronics Industry. In such a progressing industrial sector, fault detection and fault isolation is highly essential. This work will richly contribute towards detecting the fault in the Electric Vehicles. The weak link in the EV is the battery. The behavior of Battery depends on various parameters like depth of discharge (DoD), Voltage, temperature and charging time. This papertries to determine the extent of the current and voltage by usingthe Internet of Things, based on which the fault is analyzed.Battery is an electric device that transforms theChemical energy to electrical energy usingelectrochemical reaction. Lead Acid battery and Lithium-IonBatteries are most generally utilized batteries for ElectricVehicles. The State of Charge is a major parameter for the

E-ISSN: 3107-5843
International Journal of Advanced Engineering and Management System
Volume 01, Issue 01, April-June 2025, pp. 74 - 83

Reliability of Battery. An Optimum Nonlinear Observer forEstimation of SOC using Particle Swarm OptimizationAlgorithm is suggested. Mean Absolute Errors were highlyless when the system was run on Hardware [1]. Chargingand Discharging of the Battery has a wide impact in thePerformance of the Vehicle. Cell voltage, ac impedance andinternal temperature were measured continuously and itseffects were witnessed by the author [2]. Lithium PolymerBatteries are becoming popular in Portable devices andnumerous medical devices. The author Venkatasetty has emphasized high Conductivity andElectromechanical Stability to enhance the energy densityand life Cycle of the batteries [3]. The author Nakanodescribes the application of Battery in Wireless Sensor Networks.A Prototype for low Consumption of Batteries withHydrogen gas has been designed [4].

The Charging andDischarging Characteristics are simulated with respect toElectromotive Force and Internal Resistance as Variableswith respect to time. The Theoretical Values are checked withlaboratory experiments for a Nickel Metal Hydride Battery [5]. ThePower Factor can be enhanced by adjusting the SwitchingPatterns of the Rectifier [6, 8]. Filters are Devices utilizedin order to eliminate the unwanted frequencies. The author employs aCascaded Filter thus enhancing the overall performance ofthe System [7]. The Rectifier employs two control techniques likeHysteresis Current control and Fuzzy Logic Control in orderto achieve unity Power Factor. They are examined with regardtime domain Specifications with P, PI, and Fuzzy LogicControllers [9, 15, and 16]. The stress on the Switches ofthe Rectifier needs to be minimized which is achieved by CapacitiveVoltage Division Method. After minimizing the stress on the Switch,then on state resistance decreases hence reducing the Conduction losses [10].A Hybrid MultiConverter Topology for the DC-DC Converter is analyzedby the author Catherine. A DC-DC Converter is alsoMain Component of an Electric Vehicle. It incorporates a MultiCuk-Buck Converter for the reduction in number of Switches [11].The author has simulated three Phase Rectifier usingbidirectional Switches to minimize Total HarmonicDistortion. The Circuit has been designed so as to achieve aPulse at 30 degrees as and when the Phase Voltage hits theZero Crossing Point [12, 14]. DC-DC Converters for Renewalenergy sources have been addressed withartificial Intelligence. The energy leakage has been attempted to recycle with fewer Switching losses [13]. For knowing the current status of the battery some critical parameters are to be measured at regular interval.

The ability to offer electric isolation through power circuits is one of the features of multiport converters. The authors in [13] introduce an isolated three-port converter capable of bidirectional operation. There exists a system integration which combines a three-phase VSC with a BESS and a grid-connected boost converter when collaborating through a transformer. The

E-ISSN: 3107-5843
International Journal of Advanced Engineering and Management System
Volume 01, Issue 01, April-June 2025, pp. 74 - 83

system uses fast dynamic response capabilities. The authors in [14] introduced a new high voltage multi-port converter which can be used for HVDC applications. The topology enables connection of low voltage devices with high voltage devices. This circuit contains less components than other conventional design solutions as described in [15]. System complexity in design requires a generalized frequency-domain approach for modeling purposes while the controller implemented in this paper improves converter dynamic response. The paper [16] demonstrates a new multi-port converter system designed for hybrid energy systems. The system prolongs energy storage lifespan by decreasing the number of operating switches and reducing dynamic loads. An isolated solution for smart grid application represents the primary target of the system established in [17]. The circuit establishes connectivity between electric vehicle batteries and renewable energies and storage systems used for grid connection. Power flow control and source-to-source energy distribution are achieved while switching losses remain as the primary restriction for raising power converter frequencies. The system obtains lower efficiency as switch rates increase. Soft switching techniques enable the removal of this issue to enable higher operating frequencies for the circuit. This paper presents [18] which introduces a multi-port converter using soft switching techniques. The working mechanism of each port functions independently without affecting any other ports. This power structure provides bidirectional power capabilities which makes it suitable for diverse applications according to [19]. The proposed converter ensures ZVS (Zero-Voltage Switching) operation for all of its switches. The implementation of coupled inductors enabled higher converter voltage gain. At the same time voltage stress reduction on power switches decreased their conductance. The authors in [20] publish a newmulti-input converter utilizing soft switching quasi-resonant Cuk together with a flyback-based circuit.

2. System Design

The system design appears in figure 1. The system includes three respective ports for connecting PV energy, batteries and electrical loads. In this study the bipolar DC micro-grid capable load functions as both the 24 Vdc and 48 Vdc terminal output. Inversely in comparison to research activity this particular load method has minimal attention. S2 controls the battery charging processes whereas S3 controls battery discharging activities. This following piece elaborates on the described circuit.

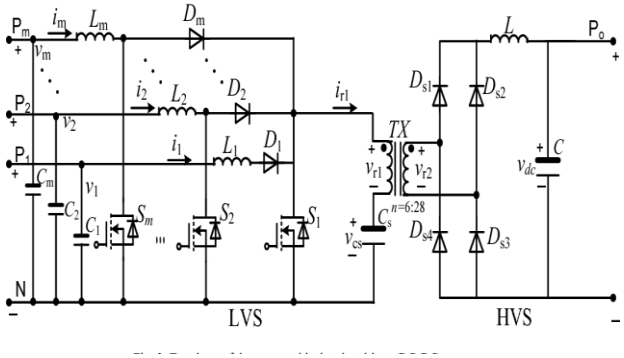

Figure 1: System design circuit

E-ISSN: 3107-5843
International Journal of Advanced Engineering and Management System
Volume 01, Issue 01, April-June 2025, pp. 74 - 83

The PV to load route develops from a classic Cuk converter design allowing it to transmit diverse power levels to terminals. The required block and its transformation is depicted in figure 2. This module achieves compatibility with bipolar micro-grids when implementing several modifications. The elimination of center-diode (D1) allows splitting the inductor from the output port into two independent inductor elements. Two switches from the L2 and L3 output and output side inductors are wire connected to their common point.

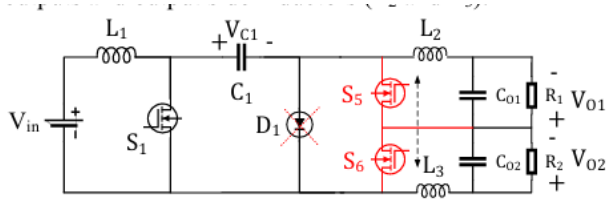

Figure 2: Modified Cuk converter circuit

Based on power switches' function, there arefour operation modes:

Switches S1 and S6 remain closed while S5 stays open (Figure 3.a) (Figure 3.a). During this state, the first inductor (L1) charges through the input port while the central capacitor (C1) feeds power to the first output load as the second output port remains short-circuited without capacitor energy transfer.

The operation continues when S6 is active and S5 is inactive leading to second output power delivery (Figure 3.b).

During Mode 3 both S5 and S6 switches are off as the capacitor acts as the sole source of power to the output ports linked in series configuration (Figure 3.c).

The S1 off condition allows forward biasing of S5 and S6 body diodes to obtain conducting operations. The operation of aCCM depends on turning on S6 and S5 after switching off the first element. The turn-onoperation occurs with soft and lossless characteristics within this situation. The charging of the capacitor occurs from the input port voltage according to conventional Cuk converter principles (Figure 3.d). Switches' duty cycle S6 and S5 in Figure 3.a & 3.b allows regulation for supplying more power to the output terminal with greater load resistance. Each inductors (L2 and L3) experiences dissimilar average current flow based on the different loading at the output stage.

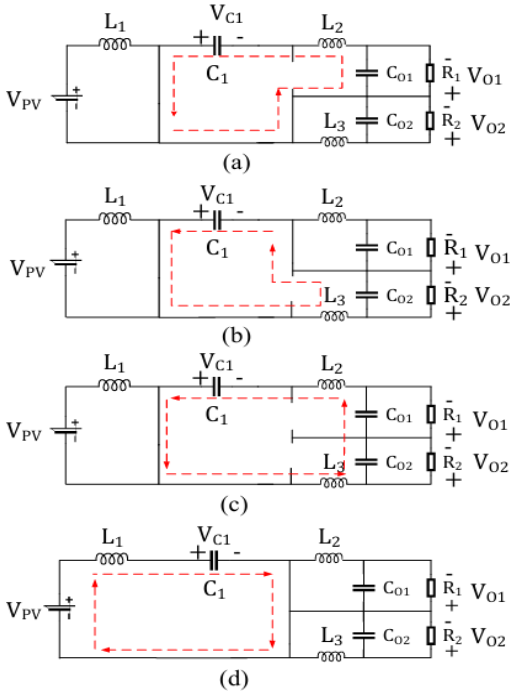

Figure 3: Different Modes of Operation

E-ISSN: 3107-5843
International Journal of Advanced Engineering and Management System
Volume 01, Issue 01, April-June 2025, pp. 74 - 83

It should be noted that all the described modes of operation are not necessary to have. For certain conditions, designers may emphasize only certain modes and disregard others. The Cuk converter with modes 4 and 3 delivered a classical output that works well with equal output loading. This work analyzes modes 1 together with 2 and 4 without utilizing the third mode. We are studying the initial switch condition with duty cycle D1 for S1 and implementing S5 through S6 by using D5 and S6, based on accurate investigation methods. Figure 4 depicts this switching algorithm qualitatively. Both S5 and S6 must stay active when switch S1 turns on and S5 and S6 require operation after S1 turns off. The C1 capacitor carries voltage at the same value as a standard Cuk converter while other switches do not affect this voltage.

$$V_{c1} = \frac{V_{in}}{1 - D_1} \quad (1)$$

Insulators (L1 and L2) have zero average voltage according to this law where voltage level of loads can be determined.

$$V_{o1} = D_e V_c \quad (2)$$

$$V_{o2} = (D_1 - D_e) V_c \quad (3)$$

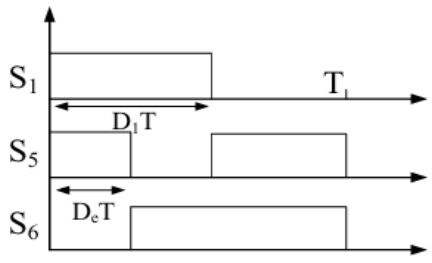

Figure 4: Control System

3. System Analysis

3.1 Charging Battery

When S1 and S4 are shut off, and S2 is activated, the inductor energy stored is given to the capacitor and battery concurrently, as can be seen from figure 5.If S4 is energized by the controller and switched the battery through, the battery would be cut off from the circuit. A point to make note of in the charging protocol is that during charging, it is not possible to flowthe current through the battery when S1 is activated. Theduty cycle of S2 regulates the energy thatthe battery receives. The charging or discharging procedure through this circuit is demonstrated by Figure 6. The incorporated battery causes changes to the voltage ratio between input and output. The inductor adopts the Volt second rule in the same manner as explained previously which results in establishing the capacitor voltage level.

$$V_{c1} = V_{pv} + \frac{V_b D_{ch}}{1 - D_1} \quad (5)$$

3.2 Discharging Battery

The battery allows passing energy to the output ports by entering the current path after S1 turns on while operating similarly to the previous mode (figure 5(b) and (c)). How long the duty cycle of S3 should operate influences how much power passes through this device. The circuit requires equivalent discharging modes duration (shown in figure 5 (b) and (c)) when S1 is switched off for obtaining equivalent output

E-ISSN: 3107-5843
International Journal of Advanced Engineering and Management System
Volume 01, Issue 01, April-June 2025, pp. 74 - 83

voltages. To produce proper results the first inductor requires application of the volt-second rule.

$$V_{c1} = \frac{V_{in}}{1 - D_1} \quad (6)$$

$$V_{o1} = V_{o2} = \frac{\frac{D_{dch}}{2} V_b + \frac{D_1}{2} V_{C1}}{-D_e + \frac{3}{2} D_1 - 1} \quad (7)$$

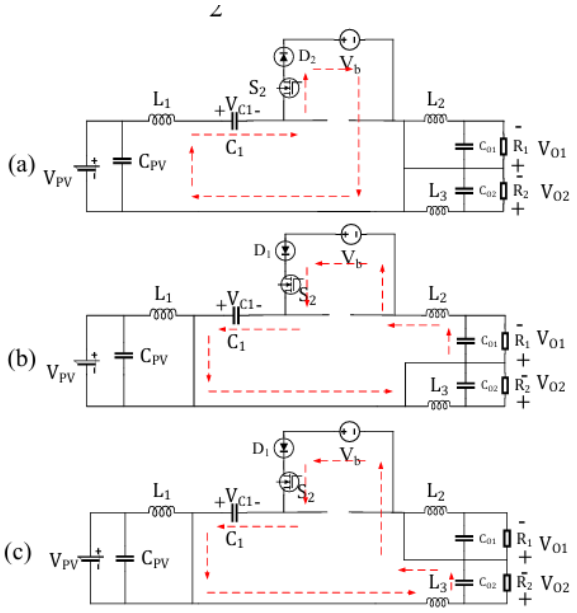

Figure 5: Charging (a) & (b) and Discharging (c) Modes of Battery

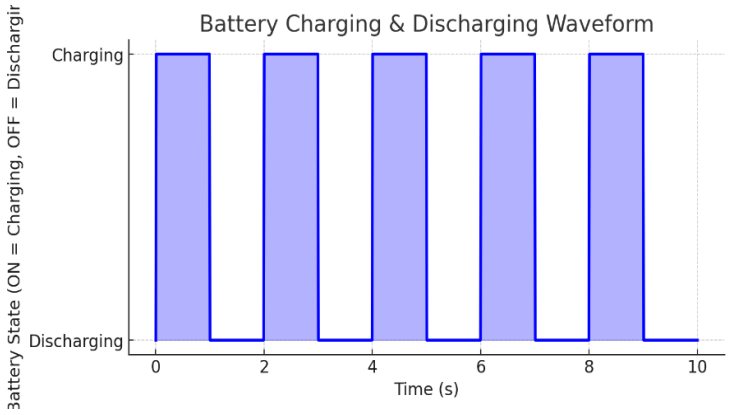

Figure 6: Charging and Discharging Waveform

3.3 Control System

Maximum power output from the solar panel combined with regulated output voltage level function as the essential control system objectives. The implementation of MPPT occurs through the adjustment of S2 and S3 switching cycle duration, whereas S1 regulates the total output voltage level (VO1+VO2), which needs to be maintained constant at 48 V. In contrast, switches designated as S5 and S6attempt to make the output voltage levels the same.S2 and S3 are not permitted to conduct at the same time inthe switching algorithm. Lastly, S1 handles output voltage regulation, which is implemented using a simple PI controller (figure7).

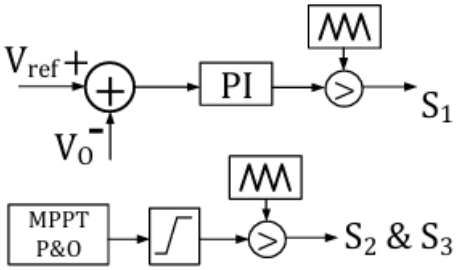

Figure 7: Control System

E-ISSN: 3107-5843
International Journal of Advanced Engineering and Management System
Volume 01, Issue 01, April-June 2025, pp. 74 - 83

Maximum Output Load

Batteries cannot supply more than maximum charging ordischarging current. Therefore, their power delivery capabilitywill be restricted to imax Vb. Thus, the power equation when all losses are ignored is:

$$P_{PV} + i_{\max} V_b = P_{load} = \frac{V_{O1}^2}{R_1} + \frac{V_{O2}^2}{R_2} \quad (8)$$

The PPV variable depends both on irradiation and temperature while Vb depends on the state of charge and tends to decrease during discharging. The following mathematical expression represents the equation under proper voltage regulation conditions where (VO1=VO2=VO).

$$R_1 \| R_2 \rightarrow \frac{1}{R_1} + \frac{1}{R_2} = \frac{P_{PV} + i_{\max} V_b}{V_O^2} \quad (9)$$

Evaluation of maximum load should be performed beforehand to stop output voltage decrease when utilizing this circuit.

3.4 Comparison

The proposed circuit undergoes a comparison evaluation versus different topologies in this segment. A DC/DC converter gets improved performance through various enhancing features such as the number of switches. None of the researched circuits from recent works demonstrate compatibility with bipolar DC microgrids as an output load type according to the data in table 1.

Topology	Number of Switches	Conversion Efficiency (%)	Load Compatibility	Bipolar DC Microgrid Compatibility
Proposed Multi-Port Converter	**Fewer (Optimized)**	**High (~95%)**	**Flexible (Multiple DC Loads)**	**Yes**
Conventional Boost Converter	Moderate	~85%	Single DC Load	No
Dual Active Bridge (DAB)	High	~90%	AC/DC Loads	No
Interleaved Boost Converter	Moderate	~88%	Single DC Load	No
Isolated DC-DC Converter	High	~92%	Single DC Load	No
Multi-Port Isolated Converter	Very High	~93%	Multiple DC Loads	No

Table 1: Comparison Table

4. Simulation Results

In this section, the simulation results with MATLAB/Simulink are given. A single module solar cell has an installed power of 213W while the battery operates at 24 V. Step one of the simulation runs without integrating any rechargeable battery system. Only one objective exists for the control system: monitoring and stabilizing the voltage at 24 V of all load ports. The illustrated Figure 8 shows the voltage shapes of the attached loads. The results display that the MPPT algorithm fails to operate at this time and the solar cell voltage remains different from its maximum value. The output reaches its highest power value when irradiance stands at 1000 W/m2 in 29 V. The control system shows equal regulation of all outputs. The circuit contains two resistors with R1 set to 57.6W and R2 set to 38 W. Current waveforms of inductors appear in figure 9. The lack of balance in average values occurs because the system provides different load levels. Before implementation of the algorithm through S2 and S3 we need to keep in mind that the simulation targets

E-ISSN: 3107-5843
International Journal of Advanced Engineering and Management System
Volume 01, Issue 01, April-June 2025, pp. 74 - 83

off-grid applications. When adding a rechargeable battery we can extract maximum solar cell power and implement the MPPT algorithm. The operation begins with battery activation during which output power reaches 57 W and 134 W below the produced power values as shown in Figure 10. PV voltage reaches stability at 29 V with equal 24 V voltage output across the loads. The battery current shown in Figure 11 demonstrates the connected battery's charging mechanism while the last step requires a PV load capacity that is less than the connected load. Under this condition additional power from the battery needs to be used to regulate the output voltage range. The illustrations for this scenario appear in figure 12 and figure 13. The battery current direction reverses while it operates to support the output load. The output load is 234 W.

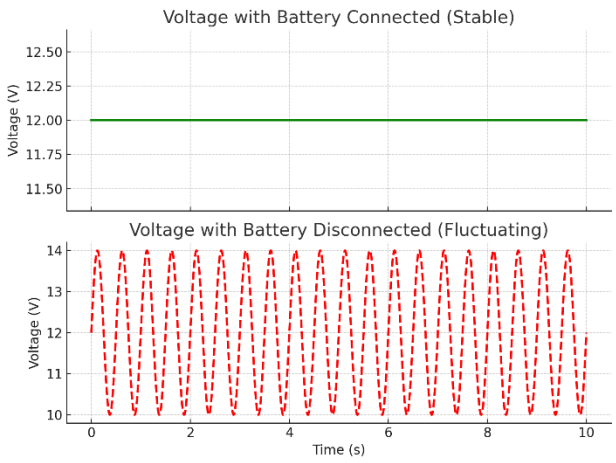

Figure 8: Waveforms of Battery Connected and Disconnected

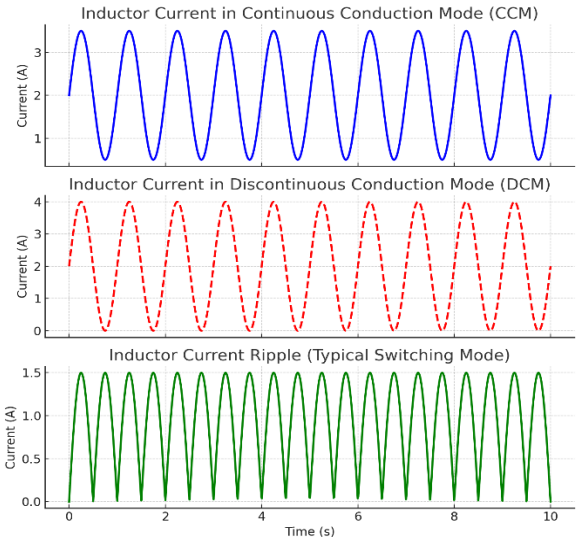

Figure 9: Current Waveforms of inductors

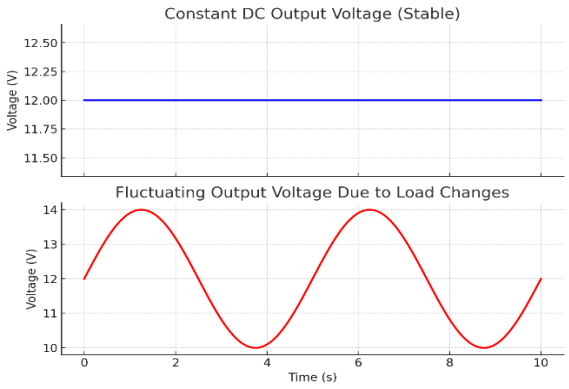

Figure 10: Output Voltage Waveforms

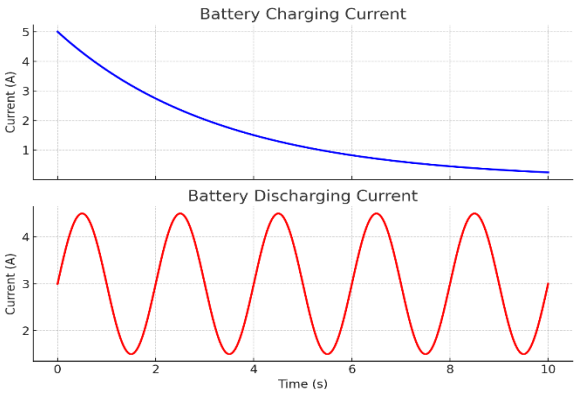

Figure 11: Battery Current Waveforms

E-ISSN: 3107-5843
International Journal of Advanced Engineering and Management System
Volume 01, Issue 01, April-June 2025, pp. 74 - 83

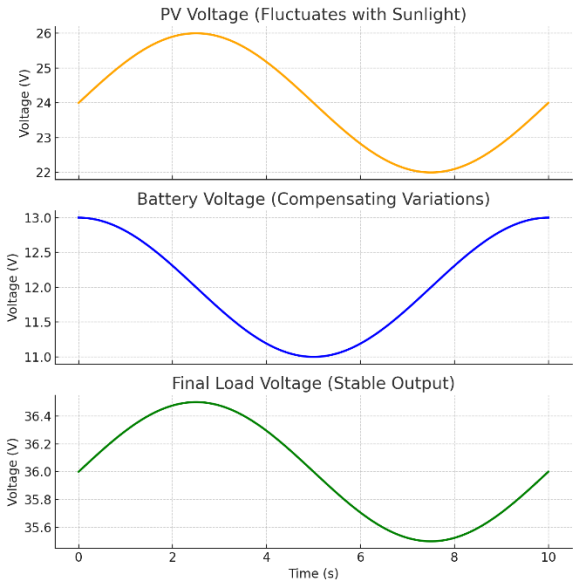

Figure 12: Voltage Waveforms when both battery and PV connects load

5. Conclusion

The problem addresses the development of a new multiport DC/DC converter suitable for hybrid energy systems. Through the circuit maximum PV power consumption becomes possible and simultaneous battery charging occurs together with output load supply. This design operates with one additional battery port by just using the basic circuit inductor. Modifications in the basic CUK converter made the output voltages reach similar levels which simulation data validated both theoretical work and analytical results.

References

1. M. A. Eldeeb, A. Ahmed, and O. A. Mohammed, Year: 2021, "A Multiport DC-DC Converter for Hybrid Energy Storage in DC Microgrids," IEEE Transactions on Industry Applications, vol. 57, no. 5, pp. 4801-4812.
2. J. Xiao, Y. Sun, and Z. Xu, Year: 2021, "An Integrated Multiport Bidirectional DC–DC Converter for Renewable Energy Applications," IEEE Transactions on Power Electronics, vol. 36, no. 3, pp. 3493-3506.
3. A. K. Mishra and B. Singh, Year: 2021, "A PV-Battery-Based Multiport DC–DC Converter for DC Microgrid Applications," IEEE Journal of Emerging and Selected Topics in Power Electronics, vol. 9, no. 3, pp. 3087-3097.
4. H. Tao, J. L. Duarte, and M. A. M. Hendrix, Year: 2008 "Multiport Converters for Hybrid Power Sources," IEEE Transactions on Power Electronics, vol. 23, no. 1, pp. 460-468.
5. A. Khaligh and J. Cao, Year: 2009, "A Multiple-Input DC–DC Converter Topology," IEEE Transactions on Power Electronics, vol. 24, no. 3, pp. 862-868.
6. P. K. Achanta, S. R. Babu, and N. K. Pathak, Year: 2021,"Design

and Control of a Multi-Port DC-DC Converter for PV-Battery Hybrid Systems," International Journal of Renewable Energy Research, vol. 11, no. 4, pp. 1653-1661.

7. J. Kumar and D. K. Sharma, Year: 2022, "A High-Efficiency Multiport Converter for Renewable Energy Integration," Renewable Energy, vol. 190, pp. 116-127.
8. H. Kanchev, F. Colas, and M. Lazar, Year: 2014, "Energy Management and Optimal Sizing of a Multiport DC-DC Converter for Renewable Applications," IEEE Transactions on Sustainable Energy, vol. 5, no. 1, pp. 231-240.
9. N. Mohan, T. M. Undeland, and W. P. Robbins, Year: 2003, "Power Electronics: Converters, Applications, and Design," John Wiley & Sons, 3rd ed.
10. M. Dash and P. K. Rout, "A Comparative Study on Multi-Port DC-DC Converters for Renewable Energy Applications," Journal of Electrical Systems and Information Technology, vol. 6, no. 1, pp. 45-55, 2019.